



Article

Integrating LCM-Based Spatio-Temporal Transcriptomics Uncovers Conceptus and Endometrial Luminal Epithelium Communication that Coordinates the Conceptus Attachment in Pigs

Feiyu Wang, Shilei Zhao, Dadong Deng, Weiwei Wang, Xuewen Xu , Xiaolei Liu, Shuhong Zhao and Mei Yu *

Key Lab of Agricultural Animal Genetics, Breeding and Reproduction of Ministry of Education, College of Animal Science and Technology, Huazhong Agricultural University, Wuhan 430070, China; feiyuw@outlook.com (F.W.); 15766387510@163.com (S.Z.); dengdadong123@sohu.com (D.D.); WeiweiWang@webmail.hzau.edu.cn (W.W.); xuewen_xu@mail.hzau.edu.cn (X.X.); xiaoleiliu@mail.hzau.edu.cn (X.L.); shzhao@mail.hzau.edu.cn (S.Z.)

* Correspondence: yumei@mail.hzau.edu.cn

Abstract: Attachment of conceptus to the endometrial luminal epithelium (LE) is a critical event for early placentation in Eutheria. Since the attachment occurs at a particular site within the uterus, a coordinated communication between three spatially distinct compartments (conceptus and endometrial LE from two anatomical regions of the uterus to which conceptus attaches and does not attach) is essential but remains to be fully characterized. Using the laser capture microdissection (LCM) technique, we firstly developed an approach that can allow us to pair the pig conceptus sample with its nearby endometrial epithelium sample without losing the native spatial information. Then, a comprehensive spatio-temporal transcriptomic profile without losing the original conceptus-endometrium coordinates was constructed. The analysis shows that an apparent difference in transcriptional responses to the conceptus exists between the endometrial LE from the two anatomically distinct regions in the uterus. In addition, we identified the communication pathways that link the conceptus and endometrial LE and found that these pathways have important roles in conceptus attachment. Furthermore, a number of genes whose expression is spatially restricted in the two different anatomical regions within the uterus were characterized for the first time and two of them (*SULT2A1* and *MEP1B*) may cooperatively contribute to establish conceptus attachment in pigs. The results from our study have implications in understanding of conceptus/embryo attachment in pigs and other large polytocous species.

Keywords: spatio-temporal transcriptomics; laser capture microdissection; endometrial luminal epithelium; conceptus attachment; pigs



Citation: Wang, F.; Zhao, S.; Deng, D.; Wang, W.; Xu, X.; Liu, X.; Zhao, S.; Yu, M. Integrating LCM-Based Spatio-Temporal Transcriptomics Uncovers Conceptus and Endometrial Luminal Epithelium Communication that Coordinates the Conceptus Attachment in Pigs. *Int. J. Mol. Sci.* **2021**, *22*, 1248. <https://doi.org/10.3390/ijms22031248>

Academic Editor: Satoshi Kishigami

Received: 13 December 2020

Accepted: 24 January 2021

Published: 27 January 2021

Publisher's Note: MDPI stays neutral with regard to jurisdictional claims in published maps and institutional affiliations.



Copyright: © 2021 by the authors. Licensee MDPI, Basel, Switzerland. This article is an open access article distributed under the terms and conditions of the Creative Commons Attribution (CC BY) license (<https://creativecommons.org/licenses/by/4.0/>).

1. Introduction

Successful embryo implantation is a critical prerequisite for establishment of placenta and ultimately determines pregnancy success rates. Collectively, the process of implantation includes two important stages: (1) initial attachment, and (2) firm attachment or invasion of the endometrium depending on the species [1,2]. Although strategies used for the second stage differ from species to species, adhesion of conceptus (embryo and associated extraembryonic membranes) to endometrial luminal epithelium (LE) is an important event that is common across species [3].

Pigs have a protracted implantation period. Conceptuses freely float in the uterus before approximately day 13 of gestation (gestation length in pigs is 114 days) [4]. Attachment of conceptus to the endometrial luminal epithelium is initiated around day 13 of gestation [5]. After a series of morphogenetic and physiological events, the attachment becomes stable by establishing a firm trophoblast-endometrial epithelial bilayer and ends with the

formation of a non-invasive epitheliochorial placenta with intact endometrial epithelium separating maternal blood and fetal membranes around days 25–30 [6]. Previous studies have identified a number of genes and signaling pathways related to conceptus attachment in pigs, such as estrogen-mediated pregnancy signaling pathways [7–11]. However, the mechanisms remain to be better understood.

Conceptus must select a particular site within the uterus for initial attachment. In the vertical direction, the uterus is demarcated into two anatomical locations: mesometrial (M) and anti-mesometrial (AM) sides, and initial attachment of pig conceptus normally takes place at the mesometrial side [12,13]. Several genes (such as *VEGF*, *IFN- γ* , *TNF- α* , *HIF-1 α* and *ABCA1*) were identified to be differentially expressed in endometrium between the two anatomical locations of the uterus during implantation in pigs [14,15]. Our recent study investigated genes and miRNAs expressed in endometrial tissues from the two anatomical locations and detected important genes and pathways that might regulate the mesometrial-biased attachment in pigs [16]. The results indicate that the molecular and physiological signatures in endometrium vary spatially within the uterus. It is worth noting that the conceptus–endometrium interface is complex and consists of heterogeneous cell types/compartments including trophoblast cells, endometrial luminal and glandular epithelial cells, stromal cells, endothelial cells and other cell types. During the attachment, conceptus produces a number of signals which directly act on endometrial epithelium or are transduced by endometrial epithelium to other compartments of the endometrium to induce endometrial receptivity [4,7,8,17]. Recent studies also revealed that genes expressed in endometrial luminal epithelium showed distinct patterns, and endometrial luminal epithelium is the main target of the conceptus signals in pigs [18,19]. Taken together, our hypothesis is that the molecular features between endometrial luminal epithelium adjacent to the conceptus (mesometrial side: M) and luminal epithelium on the opposite side of the conceptus (considered as anti-mesometrial side: AM) may be different and therefore a coordinated communication between conceptus and endometrial luminal epithelium at the two sides is of importance for successful conceptus attachment.

Spatiotemporal transcriptomics is a powerful strategy for identification of the communication pathways in tissue or organ in the natural setting [20–22]. Recently, Biase et al. [23] developed paired conceptus–endometrium analyses to determine the crosstalk at the level of an individual pregnancy in cattle. However, it is technically much more difficult to pair each conceptus with its nearby endometrial epithelium sample in large polytocous species, such as pigs. Laser capture microdissection (LCM) is a powerful technique that can capture specific single cell or tissue while maintaining the structure and spatial information [24–26]. In the present study, to provide new insight into understanding coordinated endometrial epithelium responses to the implanting conceptus, intact pig uterine samples were collected at two critical implantation stages (gestational days 12 (pre-attachment stage) and 15 (attachment stage)), respectively. Then, the LCM technique was used to dissect the endometrial luminal epithelium at the mesometrial side (LE-M), the conceptus adjacent to the LE-M and the endometrial luminal epithelium at the anti-mesometrial (LE-AM) side from the same conceptus–endometrium interface, respectively. Thereafter, spatially and temporally resolved transcriptomes were constructed and the communication pathways between conceptus and endometrial luminal epithelium from different anatomical locations of the uterus were examined.

2. Results

2.1. Transcriptomic Profiles of Three Spatially Distinct Compartments from Conceptus–Endometrium Interface in Pigs

Three spatially distinct compartments in the same uterine cross-section were laser capture micro-dissected (Figure 1). The three compartments include (1) endometrial luminal epithelium at the mesometrial side (named as LE-M) to which conceptus attaches, (2) conceptus adjacent to LE-M and (3) endometrial luminal epithelium at the anti-mesometrial side (named as LE-AM) to which conceptus does not attach. Therefore, six types of samples (3 compartments per gestational day) were used for RNA-sequencing and a total

of 15,062 genes were detected. Genes that have been reported to be expressed in pig endometrial luminal epithelium (such as *SPP1* (Secreted phosphoprotein 1) [27,28], *MUC1* (Mucin 1) [29] and *STC1* (Stanniocalcin 1) [30]) were included, and pig conceptus-expressed genes including *IFNG* (Interferon gamma) [31], *PLET1* (Placenta expressed transcript 1) [32], *PLAC1* (Placenta-specific 1) [33] and *PLAC8* (Placenta-specific 8) [34,35] were also detected. Descriptive statistics of the RNA-seq data are given in Table S1.

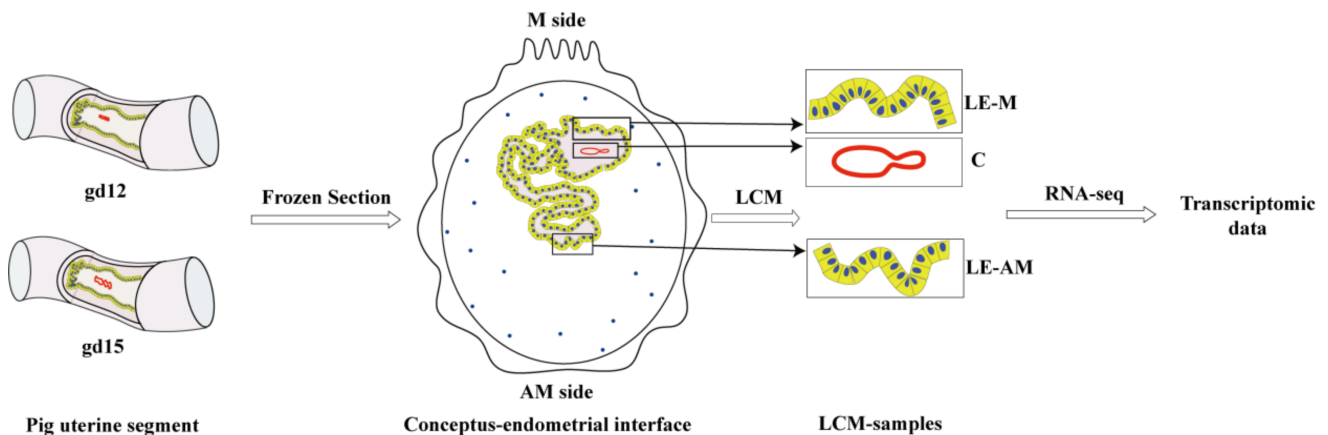


Figure 1. Schematic of the experimental workflow. Pig uterine segments in which conceptuses were not flushed out were collected from gestational days 12 (gd12, pre-attachment stage) and 15 (gd15, attachment stage) respectively, and were cross-sectioned by using a cryostat. Three spatially distinct compartments of the conceptus–endometrial interface from each stage were laser capture micro-dissected (LCM) and analyzed by RNA-seq to generate the spatial-temporal transcriptomic data. LE-M: endometrial luminal epithelium at the mesometrial side; LE-AM: endometrial luminal epithelium at the anti-mesometrial side; C: conceptuses.

2.2. Temporal Transcriptional Changes in the Three Spatially Distinct Compartments Before and at Attachment Stage

A total of 1699 and 1607 genes were detected to be differentially expressed in LE-M and LE-AM obtained between before and at the attachment stage, respectively (Figures S1 and S2; Table S2). Most of the differentially expressed genes (DEGs) were greatly enriched in terms of extracellular exosome. Of the DEGs identified in the LE-M, genes related to the integrin-mediated signaling pathway were upregulated at the attachment stage. Of the DEGs identified in the LE-AM, genes involved in carbonate dehydratase activity were upregulated, but those genes related to cell surface were downregulated at the attachment stage (Table S3). Furthermore, we identified 989 DEGs in conceptus before and at the attachment stage. The most significantly enriched GO terms were extracellular exosome and perinuclear region of cytoplasm (Figure S3; Tables S2 and S3). Therefore, the transcriptional regulation in the three spatially distinct compartments apparently differs between before and at the attachment stage.

2.3. Spatial Transcriptional Changes in LE between the Two Anatomical Locations within Uterus

Transcriptional changes between the endometrial luminal epithelium from the mesometrial side (LE-M) to which conceptus attaches and the anti-mesometrial side (LE-AM) to which conceptus does not attach were investigated. In total, 941 spatially differentially expressed genes (DEGs) were identified, in which 345 DEGs were detected in the pre-attachment stage, and 596 DEGs were detected at the attachment stage (Table S4). Most of the upregulated genes in LE-M at the two stages were mainly enriched in extracellular exosome (Figures 2 and 3; Table S5). In addition, the majority of upregulated genes in the LE-M from before and at the attachment stage were significantly enriched in apical plasma membrane and inflammatory response respectively (Figures 2 and 3; Table S5), whereas terms specific for the upregulated genes in the LE-AM at the attachment stage

were mainly related to the integral component of the plasma membrane (Figures 2 and 3; Table S5). Thus, the findings showed that at the attachment stage, molecular signatures of the endometrial luminal epithelium vary greatly by anatomical location within the uterus.

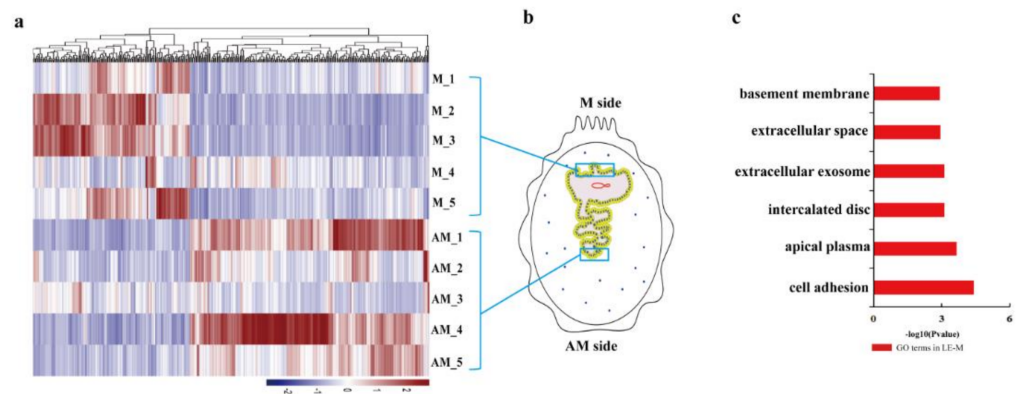


Figure 2. Heatmap and GO analysis for DEGs identified between LE-M and LE-AM on gd12 in pigs. (a) Heatmap for DEGs identified in LE-M compared to LE-AM on gd12. (b) Schematic illustration of the whole pig uterine cross-section taken from gestational day 12. (c) GO analysis of the upregulated DEGs identified in LE-M compared to LE-AM on gd12. DEGs: differentially expressed genes; LE-M: endometrial luminal epithelium at the mesometrial side; LE-AM: endometrial luminal epithelium at the anti-mesometrial side; gd12: gestational day 12 (pre-attachment stage).

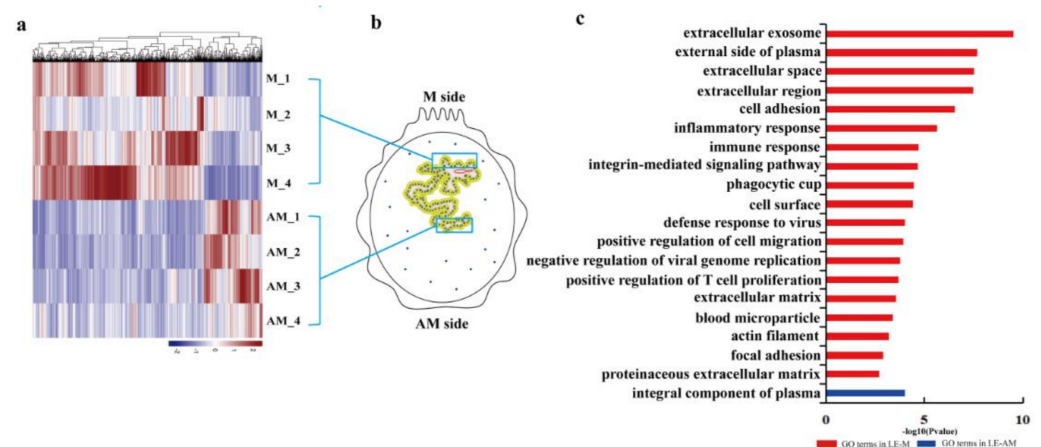


Figure 3. Heatmap and GO analysis for DEGs identified between LE-M and LE-AM on gd15 in pigs. (a) Heatmap for DEGs identified in LE-M compared to LE-AM on gd15. (b) Schematic illustration of the whole pig uterine cross-section taken from gestational day 15. (c) GO analysis of the upregulated DEGs identified in LE-M compared to LE-AM (red), and identified in LE-AM compared to LE-M (blue) on gd15. DEGs: differentially expressed genes; LE-M: endometrial luminal epithelium at the mesometrial side; LE-AM: endometrial luminal epithelium at the anti-mesometrial side; gd15: gestational day 15 (attachment stage).

2.4. Communication Pathways Linking the Conceptus and Endometrial Luminal Epithelium at the Attachment Stage

The analyses revealed the signaling pathways in which the DEGs from both conceptus and endometrial luminal epithelium participated (Table S6). Most of these pathways are related to conceptus attachment, including extracellular space, SPP1-mediated cell adhesion pathways (such as focal adhesion and integrin-mediated signaling pathway) and estrogen metabolism and signaling pathways (such as metabolic pathways and the PI3K-Akt signaling pathway) (Table S6).

2.5. Associations between Genes with Spatially Restricted Expression Patterns in LE within Uterus and Conceptus Attachment

Of the DEGs identified between the LE-M and LE-AM at the attachment stage, *SULT2A1* (Sulfotransferase family 2A member 1) and *MEP1B* (Meprin A subunit beta) are two of the most significantly differentially expressed genes. *SULT2A1* was significantly highly expressed in the LE-M; in contrast, *MEP1B* was significantly highly expressed in the LE-AM (Figure S4; Table S4). Furthermore, immunohistochemical and immunofluorescence assays were performed on the whole pig uterine cross-sectional samples from: (1) days 12 and 15 of the estrous cycle, and (2) days 12 and 15 of gestation. On days 12 and 15 of the estrous cycle, the endometrial luminal epithelium was completely negative for *SULT2A1* but contained scattered positive signals for *MEP1B*. Similarly, on day 12 of gestation (pre-attachment stage), the endometrial luminal epithelium remained negative for *SULT2A1* and showed scattered positive signals for *MEP1B* (Figure 4 and Figures S5–S12). However, on day 15 of gestation (attachment stage), *SULT2A1* was abundantly detected in the LE-M but completely absent in the LE-AM; in contrast, *MEP1B* was completely absent in the LE-M but greatly expressed in the LE-AM (Figure 5).

SPP1 is an adhesive molecule that can mediate adhesion of conceptus to the endometrial luminal epithelium [27,28,36–39]. We then examined the expression pattern of *SPP1* in the uterine cross-sections from two types of samples defined in terms of conceptus localization in the uterus: conceptus is located at the mesometrial side or away from the mesometrial side (Figure 5). The results showed that wherever the conceptus is located, *SPP1* was observed only in the endometrial luminal epithelium in close proximity to conceptus (Figure 5). The findings indicate that adhesion of conceptus can occur in different regions of the uterus in pigs. Furthermore, the expression pattern of *SULT2A1* and *MEP1B* was investigated on the two types of samples, respectively. *SULT2A1* showed exactly the same pattern as that of *SPP1* in that wherever the conceptus is located, *SULT2A1* was abundantly presented in the endometrial luminal epithelium in close proximity to conceptus but completely absent in the endometrial luminal epithelium located away from conceptus. In contrast to *SULT2A1* and *SPP1*, *MEP1B* was completely absent in the endometrial luminal epithelium in close proximity to conceptus but greatly expressed in the endometrial luminal epithelium located away from conceptus. Thus, *SULT2A1* and *MEP1B* were greatly expressed in two different anatomical uterine regions to which conceptus attaches and does not attach, respectively.

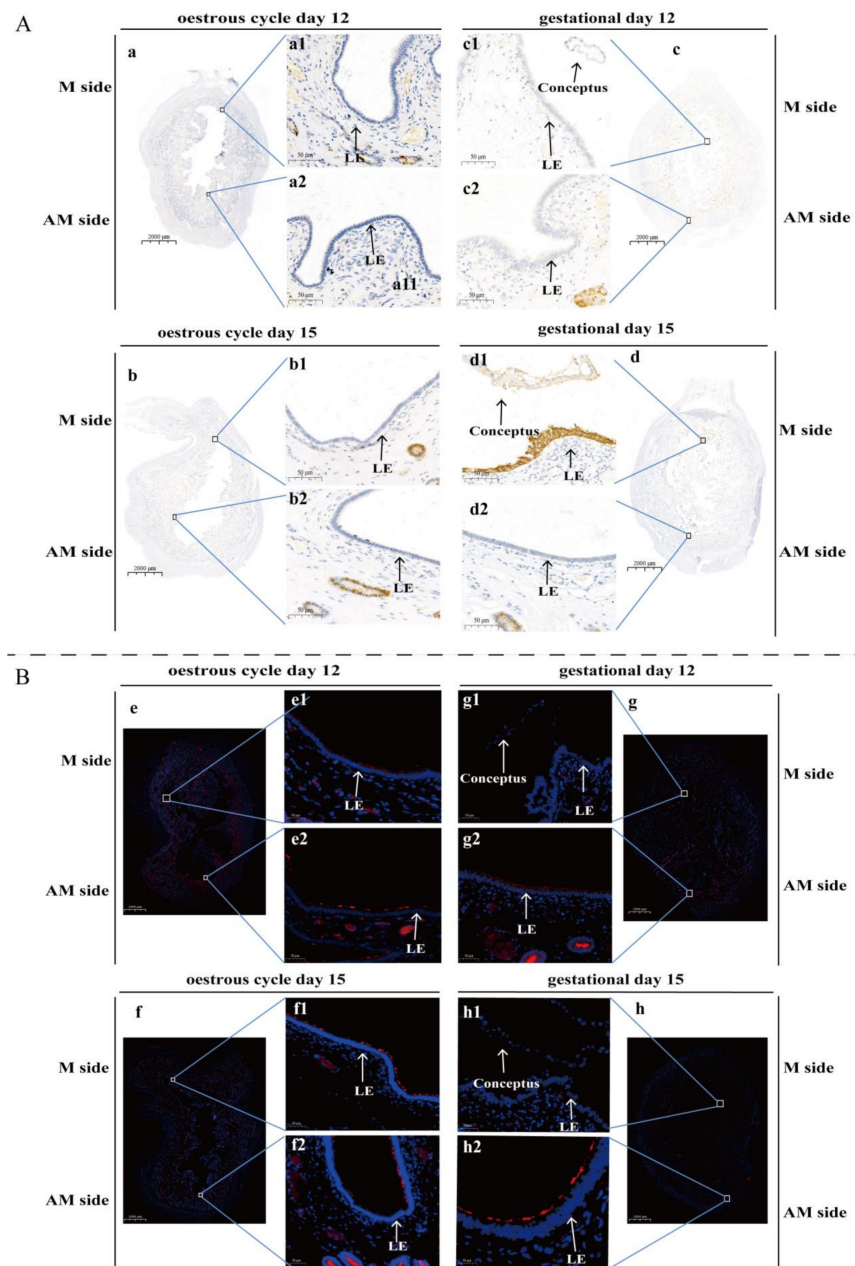


Figure 4. Spatial expression pattern of SULT2A1 and MEP1B in endometrial luminal epithelium within uterus of pigs. (A) Immunohistochemical analysis of SULT2A1 in the whole uterine cross-section of pigs ($n = 3$ gilts/estrous cycle day or gestational day). (B) Immunofluorescence analysis of MEP1B in the whole uterine cross-section of pigs ($n = 3$ gilts/estrous cycle day or gestational day). Representative images taken from the whole uterine cross-section at estrous cycle day 12 (a,e), estrous cycle day 15 (b,f), gestational day 12 (c,g) and gestational day 15 (d,h), respectively. Higher magnification images are shown of the localization of SULT2A1 in endometrial regions from the M side and AM side of the uterus respectively, and were taken from the same uterine cross-section at estrous cycle day 12 (a1,a2), estrous cycle day 15 (b1,b2), gestational day 12 (c1,c2) and gestational day 15 (d1,d2), respectively. Higher magnification images are shown of the localization of MEP1B in endometrial regions from the M side and AM side of the uterus respectively, and were taken from the same uterine cross-section at estrous cycle day 12 (e1,e2), estrous cycle day 15 (f1,f2), gestational day 12 (g1,g2) and gestational day 15 (h1,h2), respectively. LE: luminal epithelium; M side: mesometrial side; AM side: anti-mesometrial side. Scale bars = 50 μ m.

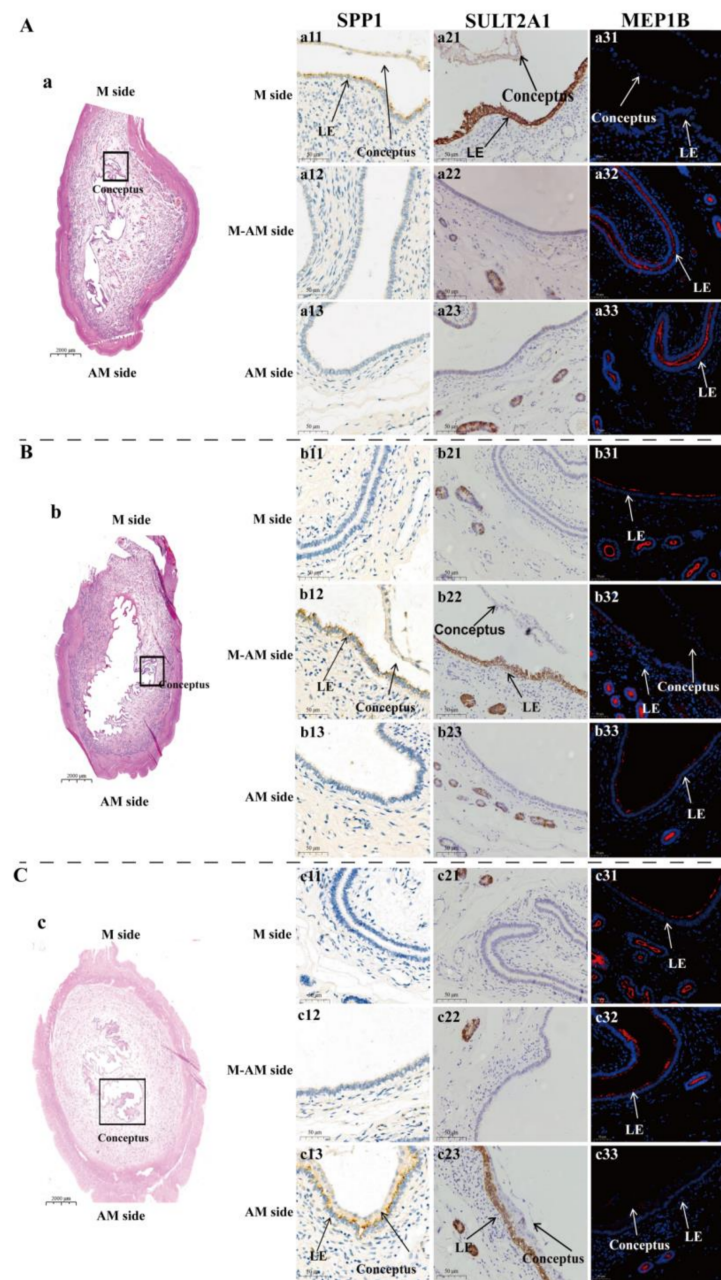


Figure 5. Expression of SPP1, SULT2A1 and MEP1B in the endometrial luminal epithelium in two types of pig uterine samples defined in terms of conceptus localization in the uterus at gestational day 15. **(A)** Representative images taken from uterine cross-section in which conceptus is located in the mesometrial side ($n = 3$ gilts). **(B,C)** Representative images taken from uterine cross-section in which conceptus is located away from the mesometrial side ($n = 3$ gilts, including uterine cross-sections in which conceptus is located between mesometrial side and anti-mesometrial side and in anti-mesometrial side, respectively.) (a–c) Hematoxylin and eosin-stained whole uterine cross-section. Higher magnification images were taken from the same uterine cross-section and show the localization of the 3 proteins in endometrial regions from the M side ((a11,b11,c11) for SPP1; (a21,b21,c21) for SULT2A1; (a31,b31,c31) for MEP1B), between M and AM side ((a12,b12,c12) for SPP1; (a22,b22,c22) for SULT2A1; (a32,b32,c32) for MEP1B) and AM side ((a13,b13,c13) for SPP1; (a23,b23,c23) for SULT2A1; (a33,b33,c33) for MEP1B) of the uterus, respectively. LE: luminal epithelium; M side: mesometrial side; AM side: anti-mesometrial side. Scale bars = 50 μ m.

3. Discussion

Synchronous communication between conceptus and the endometrial luminal epithelium surrounding the conceptus is of importance for conceptus attachment. Coupling LCM and RNA-seq techniques, we captured the conceptus and its surrounding endometrial luminal epithelium from the intact conceptus–endometrium interface at two critical implantation stages of pigs and constructed spatio-temporal transcriptomic profiles of the conceptus–endometrial luminal epithelium interface without losing the native spatial information. Then, we identified the communication pathways linking the conceptus and endometrial luminal epithelium and found that these pathways have important roles in conceptus attachment. We also characterized that genes with spatial-restricted expression patterns in the endometrial luminal epithelium may cooperate to establish the attachment of conceptus to the endometrial luminal epithelium.

The pig is a polytocous species, and it is technically difficult to establish a spatially one-to-one correspondence between a conceptus and its surrounding uterine tissue. In the present study, the intact whole uterus in which the conceptuses were not flushed out were used for cryosection. Using the LCM technique, three spatially distinct compartments (LE-M, conceptus and LE-AM) were captured from the same conceptus–endometrial interface. As expected, those genes that have been demonstrated to be expressed in porcine endometrial epithelium and conceptus were included in our datasets, respectively. In addition, some of the genes we detected are different from those reported by Zeng et al. [18,19]. The difference could be attributed to (1) the differences in pig breeds and sample collection strategies used in the two studies, and (2) the difference in samples captured since the endometrial luminal epithelium was captured separately from two anatomical regions in the uterus in the present study. Taken together, our results indicate the usability of the approach we developed in investigating the communication between conceptus and its surrounding endometrial luminal epithelium without losing the original conceptus–endometrium coordinates in pigs and other polytocous species.

A large number of DEGs were identified between pre-attachment stage and attachment stage, indicating that the expression patterns in porcine endometrial luminal epithelium differ greatly before and after conceptus attachment. In addition, of the DEGs that were identified between LE-M and LE-AM, the number of DEGs detected at the attachment stage is higher than those DEGs detected at the pre-attachment stage. The findings provided further information to show that a different response to conceptus exists between LE-M and LE-AM, and the difference became greater when conceptus attaches to the endometrial luminal epithelium [14–16]. Exosomes carry proteins, lipid and nucleic acids and participate in maternal–embryonic interaction [40,41]. Consistently, majority of the DEGs were greatly overrepresented in functional term of extracellular exosome. The genes include those that have been characterized to be involved in conceptus attachment, such as *SPP1* and *ITGAV* [4,11,27,42]. *SPP1* is an adhesive molecule that mediates porcine endometrial epithelium–conceptus adhesion through interaction with multiple integrin subunits, including *ITGAV* [43]. The findings indicate that exosomes play important roles in the conceptus–endometrial epithelium interaction during conceptus attachment in pigs, which is consistent with previous reports [18,42,44–47].

Interleukin 1 beta 2 (*IL1B2*), released specifically by pig conceptus at its elongation time (at gestational day 12, pre-attachment stage), is an alternative transcript of pro-inflammatory *IL1B* [48,49]. *IL1B2* can mediate conceptus elongation and active nuclear factor kappa-B (*NF-κB*) by upregulating *NF-κB* responsive genes (*PTGS2* and *IKBA*) in the endometrial luminal epithelium [49,50]. Consistently, *IL1B2* was only expressed in the conceptuses micro-dissected from gestational day 12 and expressions of a number of genes in the nuclear factor kappa-B (*NF-κB*) pathway were higher in the LE-M on gestational day 12. These genes include those encoding (1) interleukin 1 receptor type 1 (*IL1R1*) and interleukin 1 receptor accessory protein (*IL1RAP*), (2) three *NF-κB* subunits (*RELB*, *REL* and *NFKB2/p52*) and (3) three members of the *NF-kappa-B* inhibitor (*I-kappa-B*) family. We further found that the matrix metalloproteinase-8 (*MMP8*) gene was rapidly and transiently

induced in the endometrial luminal epithelium on gestational day 12 but undetectable on gestational day 15, indicating that an increased expression of *MMP8* in the endometrial luminal epithelium is temporally associated with the increased expression of *IL1B2* in the conceptus (Table S2). Several studies showed that *IL1B* can promote the secretion of metalloproteinases via activation of transcription factors, such as CCAAT/enhancer binding protein beta (CEBPB) [51,52]. Consistently, we found that CEBPB mRNA was also upregulated in the endometrial luminal epithelium on gestational day 12. In addition, *MMP8* belongs to the fibrillar collagenase family and plays roles in inflammation and tissue remodeling [53]. Thus, our findings suggest that, in addition to mediating the NF- κ B pathway, the increased expression of *IL1B2* in pig conceptus may also induce *MMP8* expression for endometrial luminal epithelium remodeling.

SULT2A1 is a member of the hydroxysteroid sulfotransferase subfamily and able to catalyze the sulfation of steroids, including 17 β -estradiol (E2), to the sulfate forms [54–56]. The sulfoconjugates are inactive forms of steroids and can be transported to target tissues or cells to become biologically active via the sulfatase pathway [57–59]. Previous studies have shown that estrogen sulfates were increased in the uterine fluid during implantation of pigs [60,61]. This led us to assume that the increased expression of *SULT2A1* in the endometrial luminal epithelium may play important roles in regulation of steroidogenesis and estrogen homeostasis in conceptus and the endometrial luminal epithelium. *MEP1B* is a membrane-bound metalloprotease which is involved in cleavage of several pro-inflammatory cytokines and extracellular matrix proteins and thus plays roles in regulating inflammation and tissue remodeling [62–64]. A previous study also found that *MEP1B* knockout mice have decreased litter sizes compared to wild-type litters [65]. The communication pathway analysis revealed that *SPP1*-mediated integrin pathways are related to conceptus–endometrial epithelium adhesion. In agreement with the previous reports, we found that *SPP1* and integrin subunits were upregulated on gestational day 15 in endometrial epithelium and conceptus, respectively. Pig conceptus-derived estrogens (mainly E2) are the key factors for establishment of pregnancy. The estrogens are secreted at two periods during implantation: (1) an increase in secretion between days 11 and 12 of gestation, and (2) a sustained increase in secretion from day 15 to 25 of gestation to initial attachment of conceptus to the endometrial luminal epithelium [66–68]. Previous studies showed that E2 can induce the expression of *SULT2A1* and *SPP1* but has an effect to downregulate the expression of *MEP1B*, and the effect of the estrogens is restricted to the region in close proximity to conceptus [10,35,69–71]. These results may explain the spatial-restricted expression manner of *SULT2A1* and *SPP1* in the uterus. In addition, the findings that *MEP1B* and *SPP1* exhibited spatially specific mutually exclusive patterns of expression within the uterus at the attachment stage could be explained by the previous reports that *SPP1* can be effectively degraded by *MEP1B* [62,72]. Taken together, the findings led us to hypothesize a possible model for conceptus attachment: wherever the conceptus comes into apposition, it produces estrogens to act on the endometrial luminal epithelium juxtaposed to itself and induce steroidogenesis-related genes, such as *SULT2A1*, to regulate estrogen homeostasis. At the same time, *SPP1* is induced to mediate endometrial epithelium–conceptus adhesion, and importantly, *MEP1B* is simultaneously suppressed in the same region to maintain the adhesion.

In conclusion, we constructed a comprehensive spatio-temporal transcriptomic dataset of the conceptus–endometrial luminal epithelium interface during two critical conceptus attachment stages in pigs and detected novel pathways related to conceptus attachment. Transcriptional profiles that correspond to two anatomically distinct regions in the uterus at each stage were identified and the coordinated endometrial epithelium responses to the conceptus were uncovered.

4. Materials and Methods

4.1. Sample Collection

All animal procedures were performed according to protocols approved by the Ethics Committee of Huazhong Agricultural University (HZAUSW-2016-015, 5 January 2016). Yorkshire gilts were checked for estrus twice daily and bred at the onset of the second estrus (Day 0) and again 12 h later. Uterine samples were collected on gestational days 12 (gd12, $n = 7$) and 15 (gd15, $n = 8$), respectively. The uterus was cut into 12–15 cm segments with sterile scalpel blades and numbered in sequence. Several uterine segments were randomly selected from each gilt and flushed with cold RNase-free phosphate buffer saline. If the pregnancy was confirmed by the presence of conceptuses in uterine flushings, the uterine samples without being flushed were fixed immediately in 10% neutral-buffered formalin for 24 h followed by paraffin embedding (FFPE) or embedded in precooled optimum cutting temperature (OCT) compound (SAKURA Tissue-Tek O.C.T. Compound 4583, Torrance, CA, USA), snap-frozen in liquid nitrogen and stored at $-80\text{ }^{\circ}\text{C}$. In addition, uterine samples on days 12 ($n = 3$) and 15 ($n = 3$) of the estrus cycle were collected without being flushed and further processed as described above.

4.2. Laser Capture Microdissection and RNA Library Construction

Two frozen uterine segments from each gilt (4 and 5 gilts from gestational days 12 and 15, respectively) were randomly selected for laser capture microdissection. Each segment was cross-sectioned to 13 μm -thick slices using a cryostat (Leica CM1950, Leica Biosystems, Heidelberg, Germany). The serial sections were collected and mounted onto membrane slides (MembraneSlide Nuclease and Human nucleic acid-free PEN-Membrane 2.0 μm , No.11505189, Leica). The slides were processed through a graded series of ethanol for fixation and dehydration according to a protocol reported by Chen et al. [73]. All solutions were prepared with RNase-free water. After the slides were air-dried, the laser capture microdissection was performed immediately by using a Leica LMD 7000 laser microdissection system (Leica, Frankfurt, Germany) according to the instructions. Only those sections that show the presence of conceptus were used for laser capture microdissection. In each section from each segment, the targets we captured were the endometrial luminal epithelium cells at the attachment site (mesometrial side, named as LE-M), endometrial luminal epithelium cells at anti-mesometrial to the attachment site (named as LE-AM) and conceptus. The LE-M, LE-AM or conceptus captured from the same segment were pooled. Total RNA was isolated immediately using the miRNeasy Micro Kit (QIAGEN, No. 217084, Düsseldorf, Germany) following the manufacturer's instructions.

Prior to library preparation, integrity of RNA was checked with an Agilent Bioanalyzer 2100 (Agilent Technologies, Santa Clara, CA, USA) and concentrations of RNA were determined using a NanoDrop spectrophotometer (Thermo Scientific, Waltham, MA, USA). In total, libraries were constructed using RNA yielded from each target captured from different gestational days, including 5 libraries for LE-M on gestational day 12 (1–2 segments/gilt, 3 gilts, named as gd12-LE-M), 4 libraries for LE-M on gestational day 15 (1 segment/gilt, 4 gilts, named as gd15-LE-M), 5 libraries for LE-AM on gestational day 12 (1–2 segments/gilt, 3 gilts, named as gd12-LE-AM), 4 libraries for LE-AM on gestational day 15 (1 segment/gilt, 4 gilts, named as gd15-LE-AM), 4 libraries for conceptus on gestational day 12 (1 segment/gilt, 4 gilts, named as gd12-C) and 4 libraries for conceptus on gestational day 15 (1–2 segments/gilt, 3 gilts, named as gd15-C).

4.3. RNA-Sequencing

All libraries were sequenced on the Illumina HiSeq X Ten system with a paired-end read length of 2×150 bp. The obtained clean data (Fastq files) were quality controlled with the fastQC (version 0.11.7) and 10 bp was removed from the start of the reads with the fastp (version 0.19.5) [74]. Sequences were mapped to the *Sus scrofa* genome assembly 11.1 (ENSEMBL: <ftp://ftp.ensembl.org/pub/release-96/gtf>) with Hisat2 [75] and then the duplicates were removed with samtools (version 1.9) [76]. Reads counts for each gene

from each library was calculated using HTSeq [77]. A detailed sample description is given in Table S1. Differentially expressed genes (DEGs) were determined using DESeq2 [78]. In this study, two comparisons (LE-M vs. LE-AM on gd12 and LE-M vs. LE-AM on gd15, respectively) were performed using the paired sample test to detect the transcriptional changes in the endometrial epithelium that may arise from differences in anatomical location of the uterus. The other three comparisons (LE-M from gd12 vs. LE-M from gd15, LE-AM from gd12 vs. LE-AM from gd15 and conceptuses from gd12 vs. those from gd15, respectively) were carried out using the independent sample test to detect the transcriptional changes that may arise from differences in developmental stage. The genes with adjusted p -value < 0.05 and $|\text{fold-change}| > 1$ were considered DEGs. Gene Ontology (GO) analysis for the DEGs was carried out using DAVID [79]. In addition, to investigate the communication pathways using the spatio-temporal transcriptomic dataset in which the spatial information is maintained, we combined the DEGs identified in conceptus and LE-M between stages with those DEGs detected between LE-M and LE-AM at the attachment stage. Then, the Gene Ontology (GO) analysis was performed on the combined dataset. In this study, GO terms with adjusted p -value < 0.05 were considered significantly enriched.

4.4. Quantitative Real-Time PCR

Total RNA was reverse transcribed using the PrimeScript RT Reagent Kit with gDNA Eraser (Takara Biomedical Technology, Dalian, China). The qRT-PCR was performed using standard SYBR Premix Ex Taq II (Tli RNaseH Plus) (Takara Biomedical Technology, Dalian, China) in a Bio-Rad CFX96 Touch Real-Time PCR Detection System (Bio-Rad Laboratories, Inc., Hercules, CA, USA). PCR conditions were as follows: a single cycle of 30 s at 95 °C, followed by 39 cycles of 5 s at 95 °C and 30 s at 60 °C. The gene-specific primers are listed in Table S7. The *GAPDH* gene was used as a control [80]. Wilcoxon's test was performed using R, and p -values < 0.05 were considered statistically significant.

4.5. Histologic, Immunohistochemical and Immunofluorescence Analyses

The paraffin-embedded uterine samples were cross-sectioned into 4 μm -thick slices. After deparaffinization and rehydration, the sections were stained with hematoxylin and eosin for further histologic analysis or subjected to immunohistochemical and immunofluorescence analyses.

Immunohistochemical and immunofluorescence assays were performed as previously described [15]. Briefly, the uterine cross-sections were treated with 3% hydrogen peroxide (H_2O_2) to block the endogenous peroxidase activity and then subjected to heat-induced epitope retrieval and blocked with 5% bovine serum albumin (BSA) in phosphate-buffered saline (PBS) for 30 min at room temperature. In immunohistochemical assays, sections were incubated with SULT2A1 antibody (1:100, ab194113, Abcam, Cambridge, UK) and SPP1 antibody (1:100, D121078, Sangon Biotech, Shanghai, China) at 4 °C overnight and then incubated with secondary antibody (Goat anti-rabbit IgG-Biotin, SA1022, Wuhan Boster Biological Technology, Ltd., Wuhan, China) for 30 min. Slides were developed with diaminobenzidine (DAB) and counterstained with hematoxylin and mounted using coverslips. In immunofluorescence assays, the primary antibodies used were MEP1B polyclonal antibody (1:100, CSB-PA618098ESR1HU, CUSABIO, Wuhan, China). The corresponding secondary antibodies were Cy3 conjugated Goat Anti-rabbit IgG (H + L) (red) (1:100, GB21303, Servicebio, Wuhan, China) and counterstained with DAPI (blue). For each sample, a negative control (NC) was performed by replacing the primary antibody with PBS.

All slides were scanned using the 3D HISTECH Panoramic Midi Scanner (3D HISTECH Ltd., Budapest, Hungary). The whole uterine cross-sectional images were taken and then subjected to analysis using CaseViewer software (3D HISTECH Ltd., Budapest, Hungary).

Supplementary Materials: The following are available online at <https://www.mdpi.com/1422-0067/22/3/1248/s1>.

Author Contributions: M.Y. conceived and designed the experiments; F.W. performed experiments with assistance from S.Z. (Shilei Zhao) and W.W.; F.W. performed data analysis with assistance from D.D. and X.L.; M.Y., X.X. and S.Z. (Shuhong Zhao) supervised the sample collection and analysis; F.W. and M.Y. wrote and revised the paper. All authors have read and agreed to the published version of the manuscript.

Funding: This research was funded by the National Natural Science Foundation of China (31730089, 31572370).

Institutional Review Board Statement: All animal procedures were performed according to protocols approved by the Ethic Committee of Huazhong Agricultural University (HZAUSW-2016-015, 05-01-2016).

Data Availability Statement: The RNA-seq data generated were deposited into the NCBI (national center for biotechnology information) Sequence Read Archive database (PRJNA668716).

Acknowledgments: We would like to thank Ji Huang, Yifen Yang, Miao Tian, Xihong Tan, Meng Guo, Kejia Wu, Xiaotong Wang, Sumei Hou, and Yujing Xiao for helping in sample collection and preparation.

Conflicts of Interest: The authors declare no conflict of interest.

References

1. Tinning, H.; Taylor, A.; Wang, D.; Constantinides, B.; Sutton, R.; Oikonomou, G.; Velazquez, M.A.; Thompson, P.; Treumann, A.; O'Connell, M.J.; et al. The role of CAPG in molecular communication between the embryo and the uterine endometrium: Is its function conserved in species with different implantation strategies? *FASEB J.* **2020**, *34*, 11015–11029. [[CrossRef](#)] [[PubMed](#)]
2. Namiki, T.; Ito, J.; Kashiwazaki, N. Molecular mechanisms of embryonic implantation in mammals: Lessons from the gene manipulation of mice. *Reprod. Med. Biol.* **2018**, *17*, 331–342. [[CrossRef](#)] [[PubMed](#)]
3. Aplin, J.D.; Ruane, P.T. Embryo-epithelium interactions during implantation at a glance. *J. Cell Sci.* **2017**, *130*, 15–22. [[CrossRef](#)]
4. Bazer, F.W.; Johnson, G.A. Pig blastocyst-uterine interactions. *Differentiation* **2014**, *87*, 52–65. [[CrossRef](#)] [[PubMed](#)]
5. Kyriazakis, I.; Whittemore, C. *Whittemore's Science and Practice of Pig Production*, 3rd ed.; Blackwell: Oxford, UK, 2006; pp. 105–147.
6. Friess, A.E.; Sinowatz, F.; Skolek-Winnisch, R.; Träutner, W. The placenta of the pig. I. Finestructural changes of the placental barrier during pregnancy. *Anat. Embryol.* **1980**, *158*, 179–191. [[CrossRef](#)] [[PubMed](#)]
7. Waclawik, A.; Kaczmarek, M.M.; Blitek, A.; Kaczynski, P.; Ziecik, A.J. Embryo-maternal dialogue during pregnancy establishment and implantation in the pig. *Mol. Reprod. Dev.* **2017**, *84*, 842–855. [[CrossRef](#)]
8. Ka, H.; Seo, H.; Choi, Y.; Yoo, I.; Han, J. Endometrial response to conceptus-derived estrogen and interleukin-1 β at the time of implantation in pigs. *J. Anim. Sci. Biotechnol.* **2018**, *9*, 44. [[CrossRef](#)]
9. Meyer, A.E.; Pfeiffer, C.A.; Brooks, K.; Spate, L.D.; Benne, J.A.; Cecil, R.; Samuel, M.S.; Murphy, C.N.; Behura, S.; McLean, M.K.; et al. New perspective on conceptus estrogens in maternal recognition and pregnancy establishment in the pig†. *Biol. Reprod.* **2019**, *101*, 148–161. [[CrossRef](#)]
10. Johnson, G.A.; Bazer, F.W.; Burghardt, R.C.; Spencer, T.E.; Wu, G.; Bayless, K.J. Conceptus-uterus interactions in pigs: Endometrial gene expression in response to estrogens and interferons from conceptuses. *Soc. Reprod. Fertil. Suppl.* **2009**, *66*, 321–332. [[CrossRef](#)]
11. Johnson, G.A.; Burghardt, R.C.; Bazer, F.W. Osteopontin: A leading candidate adhesion molecule for implantation in pigs and sheep. *J. Anim. Sci. Biotechnol.* **2014**, *5*, 56. [[CrossRef](#)]
12. Dantzer, V. Electron microscopy of the initial stages of placentation in the pig. *Anat. Embryol.* **1985**, *172*, 281–293. [[CrossRef](#)] [[PubMed](#)]
13. Kridli, R.T.; Khalaj, K.; Bidarimath, M.; Tayade, C. Placentation, maternal-fetal interface, and conceptus loss in swine. *Theriogenology* **2016**, *85*, 135–144. [[CrossRef](#)] [[PubMed](#)]
14. Tayade, C.; Black, G.P.; Fang, Y.; Croy, B.A. Differential gene expression in endometrium, endometrial lymphocytes, and trophoblasts during successful and abortive embryo implantation. *J. Immunol.* **2006**, *176*, 148–156. [[CrossRef](#)] [[PubMed](#)]
15. Hong, L.; Xu, X.; Huang, J.; Lei, M.; Xu, D.; Zhao, S.; Yu, M. Difference in expression patterns of placental cholesterol transporters, ABCA1 and SR-BI, in Meishan and Yorkshire pigs with different placental efficiency. *Sci. Rep.* **2016**, *6*, 20503. [[CrossRef](#)] [[PubMed](#)]
16. Huang, J.; Yang, Y.; Tian, M.; Deng, D.; Yu, M. Spatial Transcriptomic and miRNA Analyses Revealed Genes Involved in the Mesometrial-Biased Implantation in Pigs. *Genes* **2019**, *10*, 808. [[CrossRef](#)] [[PubMed](#)]
17. Kaczynski, P.; Kowalewski, M.P.; Waclawik, A. Prostaglandin F $_{2\alpha}$ promotes angiogenesis and embryo-maternal interactions during implantation. *Reproduction* **2016**, *151*, 539–552. [[CrossRef](#)] [[PubMed](#)]
18. Zeng, S.; Bick, J.; Ulbrich, S.E.; Bauersachs, S. Cell type-specific analysis of transcriptome changes in the porcine endometrium on Day 12 of pregnancy. *BMC Genom.* **2018**, *19*, 459. [[CrossRef](#)]

19. Zeng, S.; Ulbrich, S.E.; Bauersachs, S. Spatial organization of endometrial gene expression at the onset of embryo attachment in pigs. *BMC Genom.* **2019**, *20*, 895. [[CrossRef](#)]
20. Zhu, Y.; Sousa, A.M.M.; Gao, T.; Skarica, M.; Li, M.; Santpere, G.; Esteller-Cucala, P.; Juan, D.; Ferrández-Peral, L.; Gulden, F.O.; et al. Spatiotemporal transcriptomic divergence across human and macaque brain development. *Science* **2018**, *362*, eaat8077. [[CrossRef](#)]
21. Cowan, C.S.; Renner, M.; De Gennaro, M.; Roma, G.; Nigsch, F.; Roska Correspondence, B.; Cowan, C.S.; Gross-Scherf, B.; Goldblum, D.; Hou, Y.; et al. Cell Types of the Human Retina and Its Organoids at Single-Cell Resolution. *Cell* **2020**, *182*, 1623–1640.e34. [[CrossRef](#)]
22. Maniatis, S.; Äijö, T.; Vickovic, S.; Braine, C.; Kang, K.; Mollbrink, A.; Fagegaltier, D.; Andrusivová, Ž.; Saarenpää, S.; Saiz-Castro, G.; et al. Spatiotemporal dynamics of molecular pathology in amyotrophic lateral sclerosis. *Science* **2019**, *364*, 89–93. [[CrossRef](#)] [[PubMed](#)]
23. Biase, F.H.; Hue, I.; Dickinson, S.E.; Jaffrezic, F.; Laloñ, D.; Lewin, H.A.; Sandra, O. Fine-tuned adaptation of embryo-endometrium pairs at implantation revealed by transcriptome analyses in *Bos taurus*. *PLoS Biol.* **2019**, *17*, e3000046. [[CrossRef](#)]
24. Schlotter, F.; Halu, A.; Goto, S.; Blaser, M.C.; Body, S.C.; Lee, L.H.; Higashi, H.; DeLaughter, D.M.; Hutcheson, J.D.; Vyas, P.; et al. Spatiotemporal Multi-Omics Mapping Generates a Molecular Atlas of the Aortic Valve and Reveals Networks Driving Disease. *Circulation* **2018**, *138*, 377–393. [[CrossRef](#)] [[PubMed](#)]
25. Forsthofel, D.J.; Cejda, N.I.; Khan, U.W.; Newmark, P.A. Cell-type diversity and regionalized gene expression in the planarian intestine. *Elife* **2020**, *9*, e52613. [[CrossRef](#)]
26. Choi, H.; Simpson, D.; Wang, D.; Prescott, M.; A Pitsillides, A.; Dudhia, J.; Clegg, P.D.; Ping, P.; Thorpe, C.T. Heterogeneity of proteome dynamics between connective tissue phases of adult tendon. *Elife* **2020**, *9*, e55262. [[CrossRef](#)] [[PubMed](#)]
27. Garlow, J.E.; Ka, H.; Johnson, G.A.; Burghardt, R.C.; Jaeger, L.A.; Bazer, F.W. Analysis of osteopontin at the maternal-placental interface in pigs. *Biol. Reprod.* **2002**, *66*, 718–725. [[CrossRef](#)] [[PubMed](#)]
28. White, F.J.; Ross, J.W.; Joyce, M.M.; Geisert, R.D.; Burghardt, R.C.; Johnson, G.A. Steroid regulation of cell specific secreted phosphoprotein 1 (osteopontin) expression in the pregnant porcine uterus. *Biol. Reprod.* **2005**, *3*, 1294–1301. [[CrossRef](#)]
29. Ren, Q.; Guan, S.; Fu, J.; Wang, A. Temporal and spatial expression of Muc1 during implantation in sows. *Int. J. Mol. Sci.* **2010**, *11*, 2322–2335. [[CrossRef](#)]
30. Song, G.; Dunlap, K.A.; Kim, J.; Bailey, D.W.; Spencer, T.E.; Burghardt, R.C.; Wagner, G.F.; Johnson, G.A.; Wu, G. Stanniocalcin 1 is a luminal epithelial marker for implantation in pigs regulated by progesterone and estradiol. *Endocrinology* **2009**, *150*, 936–945. [[CrossRef](#)]
31. La Bonnardiére, C.; Martinat-Botté, F.; Terqui, M.; Lefèvre, F.; Zouari, K.; Martal, J.; Bazer, F.W. Production of two species of interferon by Large White and Meishan pig conceptuses during the peri-attachment period. *J. Reprod. Fertil.* **1991**, *91*, 469–478. [[CrossRef](#)]
32. Teng, L.; Hong, L.; Liu, R.; Chen, R.; Li, X.; Yu, M. Cellular Localization and Regulation of Expression of the PLET1 Gene in Porcine Placenta. *Int. J. Mol. Sci.* **2016**, *17*, 2048. [[CrossRef](#)] [[PubMed](#)]
33. Deng, D.; Hong, L.; Pan, L.; Liu, B.; Yu, M. Cloning, Tissue Expression and Inheritance Patterns of Porcine Placenta-specific1 (PLAC1) Gene. *Acta Vet. et Zootech. Sin.* **2019**, *50*, 37–43. [[CrossRef](#)]
34. Chang, W.L.; Liu, Y.W.; Dang, Y.L.; Jiang, X.X.; Xu, H.; Huang, X.; Wang, Y.L.; Wang, H.; Zhu, C.; Xue, L.Q.; et al. PLAC8, a new marker for human interstitial extravillous trophoblast cells, promotes their invasion and migration. *Development* **2018**, *145*, dev148932. [[CrossRef](#)] [[PubMed](#)]
35. Li, M.; Liu, D.; Wang, L.; Wang, W.; Wang, A.; Yao, Y. Expression of placenta-specific 8 in human oocytes, embryos, and models of in vitro implantation. *Fertil. Steril.* **2016**, *106*, 781–789.e2. [[CrossRef](#)] [[PubMed](#)]
36. Johnson, G.A.; Spencer, T.E.; Burghardt, R.C.; Bazer, F.W. Ovine osteopontin: I. Cloning and expression of messenger ribonucleic acid in the uterus during the periimplantation period. *Biol. Reprod.* **1999**, *61*, 884–891. [[CrossRef](#)] [[PubMed](#)]
37. Johnson, G.A.; Burghardt, R.C.; Spencer, T.E.; Newton, G.R.; Ott, T.L.; Bazer, F.W. Ovine osteopontin: II. Osteopontin and alpha(v)beta(3) integrin expression in the uterus and conceptus during the periimplantation period. *Biol. Reprod.* **1999**, *61*, 892–899. [[CrossRef](#)]
38. Johnson, G.A.; Spencer, T.E.; Burghardt, R.C.; Taylor, K.M.; Gray, C.A.; Bazer, F.W. Progesterone modulation of osteopontin gene expression in the ovine uterus. *Biol. Reprod.* **2000**, *62*, 1315–1321. [[CrossRef](#)]
39. Johnson, G.A.; Wu, G.; Jaeger, L.A.; Ka, H.; Garlow, J.E.; Pfarrer, C.; Spencer, T.E.; Burghardt, R.C. Muc-1, integrin, and osteopontin expression during the implantation cascade in sheep. *Biol. Reprod.* **2001**, *65*, 820–828. [[CrossRef](#)]
40. Bidarimath, M.; Khalaj, K.; Kridli, R.T.; Kan, F.W.K.; Koti, M.; Tayade, C. Extracellular vesicle mediated intercellular communication at the porcine maternal-fetal interface: A new paradigm for conceptus-endometrial cross-talk. *Sci Rep.* **2017**, *7*, 40476. [[CrossRef](#)]
41. Bridi, A.; Perecin, F.; Silveira, J.C.D. Extracellular Vesicles Mediated Early Embryo-Maternal Interactions. *Int. J. Mol. Sci.* **2020**, *21*, 1163. [[CrossRef](#)]
42. Ng, Y.H.; Rome, S.; Jalabert, A.; Forterre, A.; Singh, H.; Hincks, C.L.; Salamonsen, L.A. Endometrial exosomes/microvesicles in the uterine microenvironment: A new paradigm for embryo-endometrial cross talk at implantation. *PLoS ONE* **2013**, *8*, e58502. [[CrossRef](#)] [[PubMed](#)]

43. Erikson, D.W.; Burghardt, R.C.; Bayless, K.J.; Johnson, G.A. Secreted phosphoprotein 1 (SPP1, osteopontin) binds to integrin alpha v beta 6 on porcine trophectoderm cells and integrin alpha v beta 3 on uterine luminal epithelial cells, and promotes trophectoderm cell adhesion and migration. *Biol. Reprod.* **2009**, *81*, 814–825. [[CrossRef](#)] [[PubMed](#)]
44. O'Neil, E.V.; Burns, G.W.; Spencer, T.E. Extracellular vesicles: Novel regulators of conceptus-uterine interactions? *Theriogenology* **2020**, *150*, 106–112. [[CrossRef](#)] [[PubMed](#)]
45. Burnett, L.A.; Nowak, R.A. Exosomes mediate embryo and maternal interactions at implantation and during pregnancy. *Front. Biosci.* **2016**, *8*, 79–96.
46. Salamonsen, L.A.; Evans, J.; Nguyen, H.P.; Edgell, T.A. The Microenvironment of Human Implantation: Determinant of Reproductive Success. *Am. J. Reprod. Immunol.* **2016**, *75*, 218–225. [[CrossRef](#)] [[PubMed](#)]
47. Greening, D.W.; Nguyen, H.P.; Elgass, K.; Simpson, R.J.; Salamonsen, L.A. Human Endometrial Exosomes Contain Hormone-Specific Cargo Modulating Trophoblast Adhesive Capacity: Insights into Endometrial-Embryo Interactions. *Biol. Reprod.* **2016**, *94*, 38. [[CrossRef](#)]
48. Ross, J.W.; Ashworth, M.D.; Hurst, A.G.; Malayer, J.R.; Geisert, R.D. Analysis and characterization of differential gene expression during rapid trophoblastic elongation in the pig using suppression subtractive hybridization. *Reprod. Biol. Endocrinol.* **2003**, *1*, 23. [[CrossRef](#)]
49. Mathew, D.J.; Newsom, E.M.; Guyton, J.M.; Tuggle, C.K.; Geisert, R.D.; Lucy, M.C. Activation of the transcription factor nuclear factor-kappa B in uterine luminal epithelial cells by interleukin 1 Beta 2: A novel interleukin 1 expressed by the elongating pig conceptus. *Biol. Reprod.* **2015**, *92*, 107. [[CrossRef](#)]
50. Whyte, J.J.; Meyer, A.E.; Spate, L.D.; Benne, J.A.; Cecil, R.; Samuel, M.S.; Murphy, C.N.; Prather, R.S.; Geisert, R.D. Inactivation of porcine interleukin-1 β results in failure of rapid conceptus elongation. *Proc. Natl. Acad. Sci. USA* **2018**, *115*, 307–312. [[CrossRef](#)]
51. Librach, C.; Feigenbaum, S.; Bass, K.; Cui, T.; Verastas, N.; Sadovsky, Y.; Quigley, J.; French, D.; Fisher, S. Interleukin-1 beta regulates human cytotrophoblast metalloproteinase activity and invasion in vitro. *J. Biol. Chem.* **1994**, *269*, 17125–17131. [[CrossRef](#)]
52. Armstrong, D.A.; Phelps, L.N.; Vincenti, M.P. CCAAT enhancer binding protein-beta regulates matrix metalloproteinase-1 expression in interleukin-1beta-stimulated A549 lung carcinoma cells. *Mol. Cancer Res.* **2009**, *7*, 1517–1524. [[CrossRef](#)] [[PubMed](#)]
53. Al-Majid, A.; Alassiri, S.; Rathnayake, N.; Tervahartiala, T.; Gieselmann, D.R.; Sorsa, T. Matrix Metalloproteinase-8 as an Inflammatory and Prevention Biomarker in Periodontal and Peri-Implant Diseases. *Int. J. Dent.* **2018**, *2018*, 7891323. [[CrossRef](#)] [[PubMed](#)]
54. Nakamura, Y.; Xing, Y.; Sasano, H.; Rainey, W.E. The mediator complex subunit 1 enhances transcription of genes needed for adrenal androgen production. *Endocrinology* **2009**, *150*, 4145–4153. [[CrossRef](#)] [[PubMed](#)]
55. Thomae, B.A.; Eckloff, B.W.; Freimuth, R.R.; Wieben, E.D.; Weinshilboum, R.M. Human sulfotransferase SULT2A1 pharmacogenetics: Genotype-to-phenotype studies. *Pharm. J.* **2002**, *2*, 48–56. [[CrossRef](#)]
56. Wang, L.Q.; James, M.O. Sulfotransferase 2A1 forms estradiol-17-sulfate and celecoxib switches the dominant product from estradiol-3-sulfate to estradiol-17-sulfate. *J. Steroid Biochem. Mol. Biol.* **2005**, *96*, 367–374. [[CrossRef](#)]
57. Plager, J.E. The binding of androsterone sulfate, ethiocholanolone sulfate, and dehydroisoandrosterone sulfate by human plasma protein. *J. Clin. Investig.* **1965**, *44*, 1234–1239. [[CrossRef](#)]
58. Dooley, T.P.; Haldeman-Cahill, R.; Joiner, J.; Wilborn, T.W. Expression profiling of human sulfotransferase and sulfatase gene superfamilies in epithelial tissues and cultured cells. *Biochem. Biophys. Res. Commun.* **2000**, *277*, 236–245. [[CrossRef](#)]
59. Martel, C.; Melner, M.H.; Gagné, D.; Simard, J.; Labrie, F. Widespread tissue distribution of steroid sulfatase, 3 beta-hydroxysteroid dehydrogenase/delta 5-delta 4 isomerase (3 beta-HSD), 17 beta-HSD 5 alpha-reductase and aromatase activities in the rhesus monkey. *Mol. Cell Endocrinol.* **1994**, *104*, 103–111. [[CrossRef](#)]
60. Geisert, R.D.; Renegar, R.H.; Thatcher, W.W.; Roberts, R.M.; Bazer, F.W. Establishment of pregnancy in the pig: I. Interrelationships between preimplantation development of the pig blastocyst and uterine endometrial secretions. *Biol. Reprod.* **1982**, *27*, 925–939. [[CrossRef](#)]
61. Geisert, R.D.; Thatcher, W.W.; Roberts, R.M.; Bazer, F.W. Establishment of pregnancy in the pig: III. Endometrial secretory response to estradiol valerate administered on day 11 of the estrous cycle. *Biol. Reprod.* **1982**, *27*, 957–965. [[CrossRef](#)]
62. Jefferson, T.; Keller, U.A.D.; Bellac, C.; Metz, V.V.; Broder, C.; Hedrich, J.; Ohler, A.; Maier, W.; Magdolen, V.; Sterchi, E.; et al. The substrate degradome of meprin metalloproteases reveals an unexpected proteolytic link between meprin β and ADAM10. *Cell Mol. Life Sci.* **2013**, *70*, 309–333. [[CrossRef](#)] [[PubMed](#)]
63. Herzog, C.; Haun, R.S.; Kaushal, G.P. Role of meprin metalloproteinases in cytokine processing and inflammation. *Cytokine* **2019**, *114*, 18–25. [[CrossRef](#)] [[PubMed](#)]
64. Kronenberg, D.; Bruns, B.C.; Moali, C.; Goff, S.V.L.; Sterchi, E.E.; Traupe, H.; Böhm, M.; Hulmes, D.J.S.; Stöcker, W.; Becker-Pauly, C. Processing of procollagen III by meprins: New players in extracellular matrix assembly? *J. Investig Dermatol.* **2010**, *130*, 2727–2735. [[CrossRef](#)] [[PubMed](#)]
65. Norman, L.P.; Jiang, W.; Han, X.; Saunders, T.L.; Bond, J.S. Targeted disruption of the meprin beta gene in mice leads to underrepresentation of knockout mice and changes in renal gene expression profiles. *Mol. Cell Biol.* **2003**, *23*, 1221–1230. [[CrossRef](#)]
66. Zavy, M.T.; Bazer, F.W.; Thatcher, W.W.; Wilcox, C.J. A study of prostaglandin F2 alpha as the luteolysin in swine: V. Comparison of prostaglandin F, progestins, estrone and estradiol in uterine flushings from pregnant and nonpregnant gilts. *Prostaglandins* **1980**, *20*, 837–851. [[CrossRef](#)]

67. Fischer, H.E.; Bazer, F.W.; Fields, M.J. Steroid metabolism by endometrial and conceptus tissues during early pregnancy and pseudopregnancy in gilts. *J. Reprod. Fertil.* **1985**, *75*, 69–78. [[CrossRef](#)]
68. Joyce, M.M.; Burghardt, R.C.; Geisert, R.D.; Burghardt, J.R.; Hooper, R.N.; Ross, J.W.; Ashworth, M.D.; A Johnson, G. Pig conceptuses secrete estrogen and interferons to differentially regulate uterine STAT1 in a temporal and cell type-specific manner. *Endocrinology* **2007**, *148*, 4420–4431. [[CrossRef](#)]
69. Waclawik, A. Novel insights into the mechanisms of pregnancy establishment: Regulation of prostaglandin synthesis and signaling in the pig. *Reproduction* **2011**, *142*, 389–399. [[CrossRef](#)]
70. Thompson, C.J.; Tam, N.N.; Joyce, J.M.; Leav, I.; Ho, S.M. Gene expression profiling of testosterone and estradiol-17 beta-induced prostatic dysplasia in Noble rats and response to the antiestrogen ICI 182,780. *Endocrinology* **2002**, *143*, 2093–2105. [[CrossRef](#)]
71. Li, W.; Ning, M.; Koh, K.H.; Kim, H.; Jeong, H. 17 β -Estradiol induces sulfotransferase 2A1 expression through estrogen receptor α . *Drug Metab. Dispos.* **2014**, *42*, 796–802. [[CrossRef](#)]
72. Bertenshaw, G.P.; Turk, B.E.; Hubbard, S.J.; Matters, G.L.; Bylander, J.E.; Crisman, J.M.; Cantley, L.C.; Bond, J.S. Marked differences between metalloproteases meprin A and B in substrate and peptide bond specificity. *J. Biol. Chem.* **2001**, *276*, 13248–13255. [[CrossRef](#)] [[PubMed](#)]
73. Chen, J.; Suo, S.; Tam, P.P.; Han, J.J.; Peng, G.; Jing, N. Spatial transcriptomic analysis of cryosectioned tissue samples with Geo-seq. *Nat. Protoc.* **2017**, *12*, 566–580. [[CrossRef](#)] [[PubMed](#)]
74. Chen, S.; Zhou, Y.; Chen, Y.; Gu, J. fastp: An ultra-fast all-in-one FASTQ preprocessor. *Bioinformatics* **2018**, *34*, i884–i890. [[CrossRef](#)] [[PubMed](#)]
75. Kim, D.; Langmead, B.; Salzberg, S.L. HISAT: A fast spliced aligner with low memory requirements. *Nat. Methods* **2015**, *12*, 357–360. [[CrossRef](#)] [[PubMed](#)]
76. Li, H.; Handsaker, B.; Wysoker, A.; Fennell, T.; Ruan, J.; Homer, N.; Marth, G.; Abecasis, G.; Durbin, R.; 1000 Genome Project Data Processing Subgroup. The Sequence Alignment/Map format and SAMtools. *Bioinformatics* **2009**, *25*, 2078–2079. [[CrossRef](#)]
77. Anders, S.; Pyl, P.T.; Huber, W. HTSeq—A Python framework to work with high-throughput sequencing data. *Bioinformatics* **2015**, *31*, 166–169. [[CrossRef](#)]
78. Love, M.I.; Huber, W.; Anders, S. Moderated estimation of fold change and dispersion for RNA-seq data with DESeq2. *Genome Biol.* **2014**, *15*, 550. [[CrossRef](#)]
79. Huang da, W.; Sherman, B.T.; Lempicki, R.A. Systematic and integrative analysis of large gene lists using DAVID bioinformatics resources. *Nat. Protoc.* **2009**, *4*, 44–57. [[CrossRef](#)]
80. Pierzchała, M.; Pierzchała, D.; Ogłuszka, M.; Poławska, E.; Blicharski, T.; Roszczyk, A.; Nawrocka, A.; Urbański, P.; Liput, K.; Ciepłoch, A.; et al. Identification of Differentially Expressed Gene Transcripts in Porcine Endometrium during Early Stages of Pregnancy. *Life* **2020**, *10*, 68. [[CrossRef](#)]